Fluorescent Nanoparticles from "Hairy-Rods", Water-Self Dispersible Amphiphilic Polythiophenes

ANCA-DANA BENDREA[1], LUMINITA CIANGA[1], ELENA-GABRIELA HITRUC[1], IRINA TITORENCU[2], IOAN CIANGA[1]*

[1] "Petru Poni" Institute of Macromolecular Chemistry, 41A Gr. Ghica-Voda Alley, 700487, Iasi, Romania

[2] Institute of Cellular Biology and Pathology "Nicolae Simionescu", 8 B.P. Hasdeu Str., 050568, Bucharest, Romania

By skilful combination between polythiophene backbones and poly(ethylene glycol) (PEG) side chains of different lengths, amphiphilic, fluorescent copolymers having branched architecture of "hairy rods" type were obtained by Suzuki polycondensation. Their structural characterization was performed by ^{1}H-NMR, ^{13}C-NMR and FT-IR spectroscopies and thermal behaviour was followed by differential scanning calorimetry (DSC) and thermogravimetrical analysis (TGA). Photophysical properties in aqueous solutions were evaluated using UV-Vis and fluorescence measurements. The amphiphilic nature of the synthesized polythiophenes and the presence of PEG side chains induced the self - dispersability in water, as well as the formation of fluorescent nanoparticles through self-assembling. The size of the nanoparticles in water was assessed by dynamic light scattering (DLS) and atomic force microscopy (AFM) investigations and the effect of incubation time on three cell lines viability was evaluated, as well.

Keywords: polythiophenes, nanoparticles, Suzuki polycondensation, "hairy-rods", self-assembling

One of the most important goal at the meeting point between the nanotechnology and soft matter science is the structuring of soft materials, in particular of polymeric materials, at the nanoscale level. Nowadays, this goal becomes even more important as long as, during the past decades, the field of polymer nanoparticles is quickly expanding and play a pivotal role in a wide spectrum of areas ranging from electronics to photonics, conducting materials to sensors, medicine to biotechnology, pollution control to environmental technology, and so forth [1]. Also, the rise in the interdisciplinary study of π-conjugated polymers, essentially in parallel with nanoscience, has led to major advances in the fundamental understanding of their diverse electronic, optoelectronic, and photonic properties while enabling their applications in biomedical technology [2-4]. In contrast to intense studies on the preparation of conjugated polymers and their properties in bulk or in thin films [5-9], nanoparticles of conjugated polymers have been relatively little addressed [10-12]. As regarding fluorescence as a specific property of the conjugated polymers, it is notable that nanoparticles of the luminescent conjugated polymers received attention only more recently, the first report dating back to the past decade [11]. Fluorescent nanoparticles derived from conjugated polymers and oligomers can potentially find applications in various area, such as optoelectronics and photonics [10]. During last years, conjugated polymer nanoparticles have emerged as an attractive alternative to quantum dots, as useful materials for bioimaging / biosensing agents or as nanomedicines, as they combine the advantages of inorganic particles with those of micelles and vesicles, thus creating stable, highly- fluorescent and highly photostable dynamic particles [12]. Mainly, two techniques are used for the preparation of conjugated polymers nanoparticles: (i) postpolymerization dispersion and (ii) polymerization in heterophase systems [11]. Conjugated polymer nanoparticles can be prepared, as well, by self-assembly of amphiphilic π-conjugated rod – coil copolymers [12]. One of the most significant features of the rod-coil amphiphiles comes from their unique anisotropic molecular shape, the main driving force behind the self-assembly in water being the strong aggregation tendency due to the π -π stacking interactions, the hydrophilic/hydrophobic balance and solution conditions, factors which enabled the construction of controllable, well-defined, highly versatile and dynamic nanostructures [13]. Moreover, the supramolecular shapes of the formed aggregates in water can be manipulated by the variation of rod-coil copolymer type, namely the linear, star or comb-shaped macromolecular architecture. On the other hand, the design of macromolecules described as "hairy rods" proved to be particularly successful and novel types of supramolecular architecture were obtained, these ones being described as "molecularly reinforced liquids" [14-16]. Launced by G. Wegner, the "hairy-rod" concept, based on the introduction of conformationally mobile, relatively long and flexible side chains to the rigid, conjugated polymer backbone, benefit from the development of the of the new polymerization methods, notably of controlled free radical polymerizations, which facilitated the synthesis of various new "hairy-rods", especially using "macro-monomer technique" [17, 18]. Thiophene-based materials present all aspects of a rich and homogeneous family of conjugated compounds, such type of π-conjugated materials being used as active components in organic light emitting diodes (OLEDs), organic field-effect transistors (OFETs), integrated circuits and organic solar cells (OSCs) [19]. From the biological activity point of view, thiophene is one of the most important heterocycles, widely used as building blocks in many pharmaceuticals [20]. Moreover, the naturally occurring α-terthienyl, a secondary metabolite extracted from the root of Marigold (*Tagetes erecta Asteraceae*), works as a singlet oxygen sensitizer, its light-mediated cytotoxic, antibacterial, antifungal, anti-HIV or insecticidal activities being reported [21]. Recently, water soluble fluorescent oligo- and polythiophenes of polyelectrolytes type were used for *in vitro* non-specific cellular imaging and anticancer activity [22, 23] or as active

* *email: ioanc@icmpp.ro*

reagents in cancer photodynamic therapy [24]. Following our previous interest in the thiophene-containing monomers and polymers with designed architectures and tuned photophysical properties [25-29], the present work reports on the synthesis of two amphiphilic structures based on PEG as side chains and poly(thiophene-2,5-diyl) main chains, synthesized *via* "macromonomer technique" in conjunction with Suzuki polycondensation. In the light of the recent obtained results [30-32], we expect that these new amphiphilic polythiophenes, due to the structural peculiarities, could self-assemble in water as "stealth" nanoparticles with a biocompatible PEG corona and a fluorescent core, leading to useful materials for both cell-imaging and photodynamic therapy.

Experimental part

Materials

Poly(ethylene glycol) methyl ether Mw = 1000 (PEG 1000) and poly(ethylene glycol) methyl ether Mw = 2000 (PEG 2000) (Aldrich), 3-thiophene carboxylic acid (Aldrich), 2,5-tiophenediboronic acid (Aldrich), N,N'-dicyclohexyl-carbodiimide (DCCI) (Merk), 4-dimethylamino pyridine (DMAP) (Aldrich), $Pd(PPh_3)_4$ (Sigma-Aldrich) were used as received. All solvents were purified and dried by usual methods. 3-(4,5-dimethylthiazol-2-yl)-2,5-diphenyl tetrazoliumbromide (MTT) was purchased from (Sigma-Aldrich), cell culture supplies including Dulbecco's Modified Eagle Medium (DMEM from Sigma Aldrich), fetal calf serum (FCS) (PAA Laboratories GmbH), Newborn Calf Serum (NCS) (PAA Laboratories GmbH); and penicillin/ streptomycin (P/S) being purchased from (PAA Laboratories GmbH).

Measurements

NMR spectra were recorded at room temperature on a Bruker Avance DRX-400 spectrometer (400 MHz), as solutions in acetone-d_6, $CDCl_3$ or DMSO-d_6 and the chemical shifts are reported in ppm and referenced to TMS as internal standard. The relative molecular weights were determined by gel permeation chromatography (GPC), using a PL-EMD instrument, polystyrene standards for the calibration plot and $CHCl_3$ or THF as elution solvents. FT-IR spectra were recorded on a Bruker Vertex 70 FTIR spectrometer, equipped with a diamond ATR device (Golden Gate, Bruker) in transmission mode, by using KBr pellets. UV-Vis and fluorescence measurements of the compounds solutions (0.01 mg/mL) were carried out by using water as solvent on a Specord 200 spectro-photometer and Perkin Elmer LS 55 apparatus, respectively. DSC experiments were conducted on a Maia DSC 200 F3 apparatus (Netzsch, Germany) under nitrogen. TGA analysis were performed on an STA 449 F1 Jupiter equipment (Netzsch, Germany) with a scanning rate of 10 °C/min. Dynamic light scattering (DLS) measurements were conducted using a Zetasizer Nano ZS90 (Malvern) apparatus, equipped with a 4.0 mW He-Ne laser, operating at 633 nm, and an avalanche photodiode detector. Measurements were carried out at 25 °C on filtered aqueous solutions of nanoparticles (0.01 mg/mL). Atomic Force Microscopy (AFM) images were registered in air, on a SPM SOLVER Pro-M instrument. A NSG10/Au Silicon tip with a 35 nm radius of curvature and 255 kHz oscillation mean frequency, was used. The apparatus was operated in semi-contact mode, over a 10 x 10 μm^2 scan area, 256 x 256 scan point size images being thus obtained. The films were prepared by drop casting from polymers aqueous solution (0.01 mg/mL) onto a freshly cleaved mica support, followed by lyophilization.

Cell culture

MG63 osteoblast-like cells were seeded onto 96 well plates at 25×10^3 cells/cm^2 density and cultured in Dulbecco's Modified Eagle Medium (DMEM) with 1‰ glucose supplemented with 10% heat-inactivated fetal bovine serum (FBS), 100 U/l penicillin, 100 U/l streptomycin and 50 U/l neomycin. Cell cultures were sustained at 37 °C under a humidified atmosphere of 5 % CO2 and 95 % air. The HTB11 (neuroblastoma cell line derived from human bone marrow) and HTB14 glioma cell line were seeded onto 96 well plates at the same density as MG63 and cultured in Dulbecco's Modified Eagle Medium (DMEM) with 1‰ glucose supplemented with 10 % fetal bovine serum (FBS), 100 U/l penicillin, 100 U/l streptomycin and 50 U/l neomycin.

Cell Viability

Cell viability was determined by MTT (Sigma Germany) assay - a colorimetric method for the determination of cell densities [33]. The assay is dependent on the cleavage of the yellow tetrazolium salt to the purple formazan crystals by metabolic active cells. Because tetrazolium salts are reduced to the colored formazan only in the presence of metabolically active cells, these assays exclusively detect viable cells. The cells on 96 well plates were cultured in medium supplemented with polymers and were incubated with 0.5 mg/mL of MTT for 4 h. Then the medium was decanted, formazan salts were dissolved with 0.1 N HCl in anhydrous isopropanol and the optical density of the formazan solution was read on a TECAN 96-well plate reader. Cells grown only in culture medium were used as positive control, the results being expressed as viability percentage.

Synthesis

Synthesis of 2,5-dibromothiophene-3-carboxylic acid

The reaction was performed using a method adapted from literature [34].

^{1}H-NMR ($CDCl_3$): 10.86 ppm (COO*H*), 7.4 ppm (Ti*H*).

Synthesis of PEG macromonomers functionalized with 2,5 dibromothiopene moieties (**1**,**2**)

8 g (0.004 mol) of PEG 2000, and 1.716 g (0.006 mol) of 2,5-dibromothiophene-3-carboxylic acid were placed into a three-neck round-bottom flask equipped with a dropping funnel, under N_2. 70 mL of CH_2Cl_2 and 0.0726 g (0.00006 mol) DMAP were added to the flask. 1.2312g (0.006 mol) DCCI in 6 mL CH_2Cl_2 were placed in the dropping funnel and added in about 15 min. The mixture was stirred at room temperature for three days. The resulting solution was filtered and precipitated in cold diethyl ether to remove the catalyst and unreacted reagents. After filtration and drying (**1**) was obtained as white solid. (**2**) was synthesized in a similar manner using 8 g (0.008 mol) of PEG 1000, 3.432 g (0.012 mol) of 2,5-dibromothiophene-3-carboxylic acid, 0.1452 g (0.0012 mol) of DMAP and 2.4624 g (0.012 mol) of DCCI.

FT-IR (**1**), (**2**) (KBr, cm^{-1}): 3091, 2884, 2738, 1728, 1524, 1464, 1423, 1359, 1342, 1277, 1241, 1148, 1112, 1059, 1005, 964, 765, 497.

General procedure for synthesis of PEG substituted polymers by Suzuki polycondensation

A 100 mL three necks round bottom flask equipped with a condenser, a septum, nitrogen inlet-outlet; and magnetic stirrer was charged with 20 mL 1M $NaHCO_3$ solution and 30 mL of THF. The solvents were previously degassed by

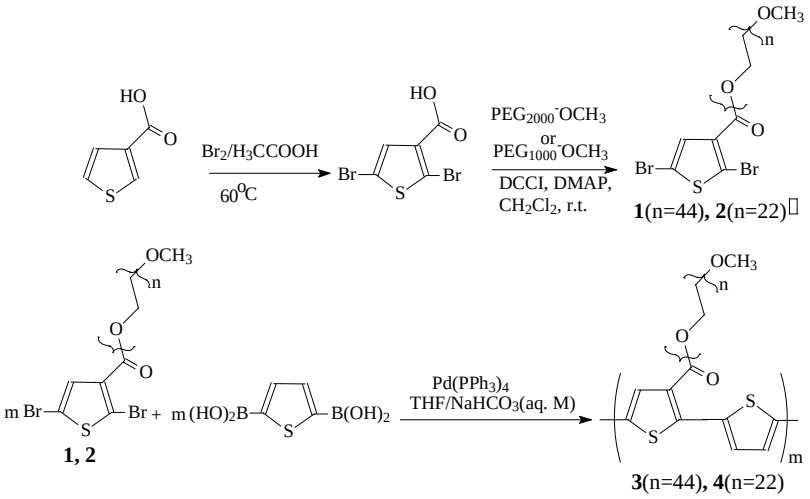

Scheme 1. Synthesis of thiophene-functionalized PEG macromonomers and of the amphiphilic polythiophenes with a "hairy-rods" architecture

bubbling nitrogren over a period of 30 min . The mixture was refluxed under nitrogen for 4 h. A 20 mL three necks round bottom flask equipped in the same way as the previous one was charged under inert atmosphere with 0.78 mmol PEG macromonomer (**1** or **2**), 0.1 mmol 2,5-tiofenediboronic acid and 0.0135 g (0.0117 mmol) $Pd(PPh_3)_4$. 3.5 mL of the mixture of solvents were introduced with a syringe through the septum. The reaction was maintained at reflux, under vigorously stirring and with the exclusion of oxygen and light. After 4 days, the reaction mixture was diluted with THF and the mixture of solvents (THF/water) was removed under vacuum at rota-evaporator. The obtained polymer (**3** or **4**) was dissolved in CH_2Cl_2, filtered and precipitated in cold diethyl ether. Further purification was achieved by passing the polymer through a silicagel column using CH_2Cl_2 as eluent followed by reprecipitation in diethyl ether.

FT-IR (**3**): (KBr, cm^{-1}): 3435, 2888.3, 2739, 2694, 1723, 1651, 1560, 1468, 1414, 1359, 1344, 1280, 1242, 1146, 1114, 1060, 963, 947, 842, 529, 511.

(**4**): 3429, 2873, 2753, 2695, 1961, 1715, 1642, 1466, 1455, 1414, 1351, 1281, 1249, 1106, 1040, 951, 884, 842, 531.

Results and discussions

Synthesis and structural characterization

The strategy for the synthesis of PEG-substituted polythiophenes is shown in scheme 1. 2.5-Dibromo-thiophenes substituted at position 3 with PEG of different size length were obtained in two reaction steps. 2,5-Dibromothiophene-3-carboxylic acid was synthesized by bromination of 3-thiophene carboxylic acid. Macro-monomers (**1**) and (**2**) were obtained by using chain-ends functionalization method, through the condensation reaction between commercially available PEG 2000 and PEG 1000 with 2,5-dibromothiophene-3-carboxylic in the presence of DCCI (scheme 1) [32].

In order to assure the complete conversion of the hydroxyl functionality of PEGs, high excess of 2,5-dibrominated 3-thiophene carboxylic acid was used. ^{1}H-NMR spectrum of (**1**) in acetone-d_6 confirms the proposed structure (table 1). The ratio of the integrals from 7.46 ppm (thiophene protons) or from 4.41 ppm (CO-OCH_2,) to that from 3.29 ppm (OCH_3) is of 1/3 or 2/3, respectively, as expected. The GPC traces of the macromonomers (**1**) and (**2**) (table 1) were unimodal and narrow and show slightly higher values of the molecular weight Mn and of the polydispersity index (PDI) as compared with the starting commercially PEGs (e.g., using THF as eluent, $Mn_{,1}$ = 2743 and PDI = 1.05 as compared to PEG 2000 having Mn = 2543 and PDI = 1.03 and $Mn_{,2}$ = 1295 and PDI = 1.04 as compared to PEG 1000 having M_n = 1125 and PDI = 1.06). This difference is certainly due to the new introduced 2,5-dibromotiophene moiety in the macromonomers structures. As can be observed in table 1, the GPC values for Mn and PDI obtained using $CHCl_3$ as eluent are higher

Structure	Code	Mn_{GPC}; PDI		Colour	^{1}H-NMR (acetone-d_6) (δppm)
		THF	$CHCl_3$		
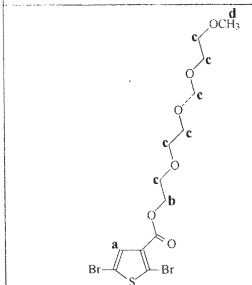	**1**	2767; 1.05	3034; 1.20	white	acetone-d_6:7.46 (**a**), 4.41 (**b**); 4-3.36(**c**), 3.28 (**d**)
	2	1208; 1.05	1414; 1.20	white	acetone-d_6:7.45 (**a**), 4.42 (**b**); 3.85-3.44 (**c**) 3.39 (**d**)
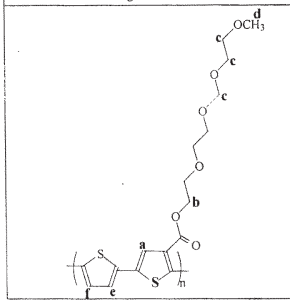	**3**	21870; 1.22	23200; 1.24	yellow	DMSO-d_6: 7.48 (**f**); 7.18 (**a**); 7.00 (**e**); 4.58 (**b**); 3.7-3.15 (**c,d**)
	4	13850 1.31	15730 1.34	light brown	acetone-d_6: 7.67 (**f**);7.52(**a**); 7.17 (**e**); 4.36 (**b**); 3.8-3.43 (**c**); 3.4 (**d**)

Table 1
GPC AND ^{1}H-NMR DATA OF MACROMONOMERS AND COPOLYMERS

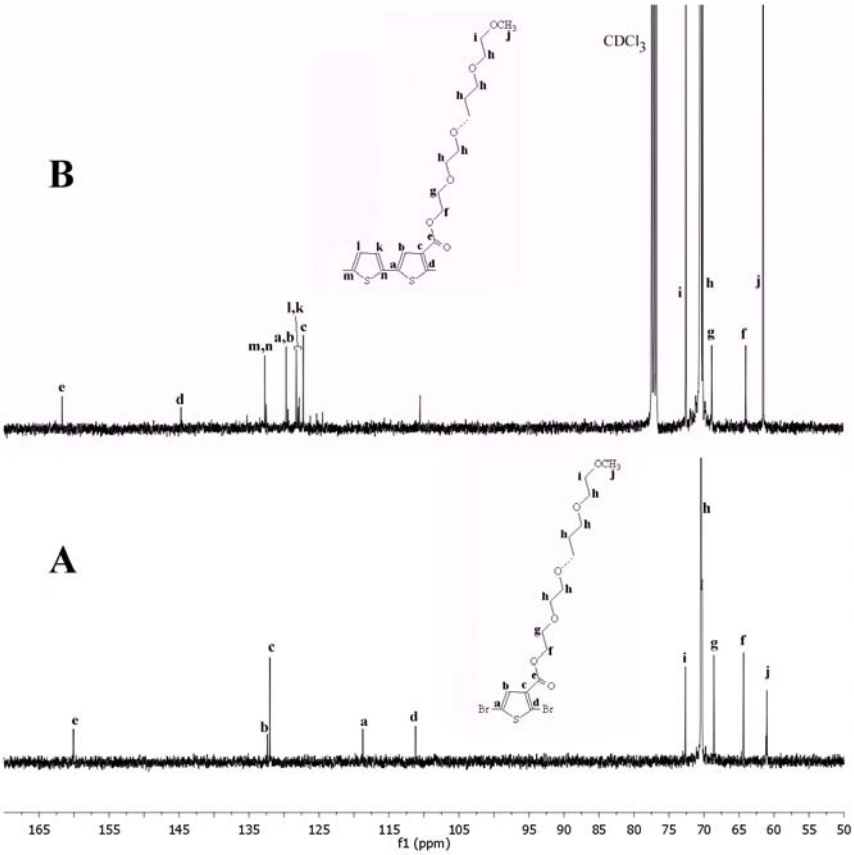

Fig. 1 ^{13}C-NMR spectrum of (**2**) (A) in acetone-d_6 and of (**4**) (B) in $CDCl_3$

than those obtained when THF was used. Generally, the GPC measurements of PEGs using columns calibrated with PSt standards furnish overestimated values of molecular weights due to the difference in polarity between these two polymers. On the other hand, if the molecular weight calculation based on the presence of the end groups in ^{1}H-NMR is attempted, the integral value of CH_2O protons in PEG branch must be used. Some errors could appear in such calculation due to the eventually presence of inherently PEG bonding water or water traces from the used solvent for the NMR registration. The protons from such water traces appear in ^{1}H-NMR spectrum in the same region as CH_2O protons in PEG, that can affect the overall value of this integral. Consequently, in our further calculations we assumed theoretical values of M_n = 2268 for (**1**) and M_n = 1268 for (**2**).

In the last synthesis step, macromonomers (**1**) and (**2**) were used in Suzuki type polycondensation reactions in combination with commercially available 2,5-thiophene diboronic acid in accordance with scheme 1. Polytiophenes (**3**) and (**4**) resulted as coloured products. This behaviour is interesting taking into account that the starting PEGs are white and they represent about 80-90 % in the resulted copolymers. These copolymers have similar solubility as PEG itself, including water.

The molecular weights of (**3**) and (**4**) measured by GPC based on polystyrene standards and listed in table 1 should be taken as a minimum estimation due to the comb-like structure of the obtained polymers. It is interesting to note that the GPC traces of the polymers are slightly broader, but still symmetrical. The differences observed for the M_n and PDI values obtained using THF or $CHCl_3$ as eluents can be due to the different behaviour of the obtained co-polymers in these two solvents. Since $CHCl_3$ is a good solvent for both main chain and PEG side chains, most probably the aggregation of the macromolecular chains in this solvent and supramolecular entities formation are suppressed. THF is a good solvent for polythiophenes main chains, while for PEG is a moderately good solvent [35]; therefore the copolymers aggregation can be taken into account for the different values of M_n and PDI. ^{1}H-NMR spectra of both macromonomers and polythiophenes confirms the proposed structures. The structural molecular formula and the protons peaks assignments are given in table 1. The ratio between the integrals of aromatic protons and the peak from around 4.5-4.3 ppm is 1/2 in case of macromonomers (**1**) or (**2**) and 2/3 in case of copolymers (**3**) or (**4**), as expected. The structures of both macromonomers and resulted copolymers were also confirmed by ^{13}C-NMR analysis. In figure 1A is presented the ^{13}C-NMR spectrum of the macromonomer (**2**). The signals specific to PEG component were identified in the 75-60 ppm region. The peaks **a**, **b**, **c**, and **d** of the carbon atoms in thiophene ring appeared in the range 111 ppm - 132.50 ppm. The signal at 161 ppm is due to the presence of the carbonyl from the ester functionality. The ^{13}C-NMR spectrum of (**4**) in $CDCl_3$ (fig. 1 B) shows more peaks in the aromatic region (144.6 ppm, 132.7-132.5 ppm, 129-7-129.4 ppm, 128.3-127.8 ppm, 127.2 ppm) by comparing with the macromonomer (**2**), due to the presence of several types of carbon atoms in the repeating unit of polytiophene (**4**).

The presence of a peak at 110 ppm could be due to the chain ends. The peak from 161.7 ppm is attributed to the carbonyl group in the ester function between thiophene ring and PEG side chains. Peaks from 72.7 ppm, 71.3-69.3 ppm, 68.8 ppm, 64.1 ppm and 61.3 ppm are specific to PEG component and their attribution are shown in figure 1 B. The structures of all synthesized compounds were also confirmed by FT-IR spectroscopy, the characteristic signals for PEG side chains, ester functionality and polythiophenes main chains being given in the experimental part.

Thermal behaviour

The thermal behaviour of macromonomers (**1**, **2**) and the corresponding polythiophenes (**3**, **4**) was followed in comparison with the starting PEG 2000 and PEG 1000 by

Polymer	IDT(°C)	T_{w10} (°C)	Y_{C800} (%)	M.p.(°C)
PEG2000	311.7	382	4.8	54.4
1	259	349	0	52.2
3	350	375	3.6	54.9
PEG1000	317	376	1.1	43.1
2	230	340	0	39.4
4	289	337	2.6	41.4

IDT – initial degradation temperature, T_{w10} – The temperature for which the weight loss is 10%

Y_{C800} – The percent of char yield at 800 °C, M.P.- Melting point (from DSC)

Table 2
THE THERMAL DATA OF COMPOUNDS

Code	λ_{max} abs. nm	λ_{max} emis.[b] nm	Stokes shift (cm^{-1})	Diameter(nm)[c]
3	***248***; ***314***; 374	***442***	9223	130
4	***326***; 506; 520	***460***	8935	91.3

a - The bold, italicized wavelength is the band maximum, the other values being present in the spectra as shoulders; b - λexcitation = λ_{max} abs; c - Determined by DLS measurements.

Table 3
PHOTOPHYSICAL PROPERTIES[A] OF POLYTHIOPHENES AND THEIR DLS DATA IN WATER

TGA and DSC analysis. The experimental data are presented in table 2. The values for IDT and T_{w10} found for starting PEGs, are lower in case of the macromonomers, while increased values were obtained for the polythiophenes. On the other hand, from the TGA data (table 2) can be noticed that the polymers containing PEG 2000 substitutes have slightly higher thermal stability than those containing PEG 1000. Melting points determined from DSC measurements have higher values in case of the starting materials as compared with the macromonomers.

When the thiophene ring is linked at one end of the PEG chains, the length of crystallization is shortened leading to lower melting points temperatures. In the case of polythiophenes, these values are increased again due to the rigid nature of the conjugated chain that favours the alignment of the lateral PEG chains.

Photophysical properties of polythiophenes in aqueous solutions

UV-vis and fluorescence spectra of polythiophenes (**3**) and (**4**) were recorded in water solutions at the same concentration. The results are presented in table 3 and figure 2. Higher intensities are noticed for both the absorption and emission maximum in case of polymer (**4**) containing PEG 1000 as substitutes, as compared with (**3**). The result seems natural as long as in the similar amount of polymers the "concentration" of the conjugated polythiophene backbone, which is the main responsible for the optical properties, is about two times higher than that in the case of (**4**) which has as substitutes PEG 2000.

It is worth to mention, as well, that both polymers show blue fluorescence under UV light. As exhibited in figure 2, both absorption and emission spectra are broad, asymmetric in shape, with vibronic fine structure, red shifted shoulders relative to the main peaks and long red tails, features that usually were attributed to the aggregations that are taking place during the nanoparticles formation [11,12]. They appear as a consequence of a multitude of main chain conformations and locally variable degrees of order.

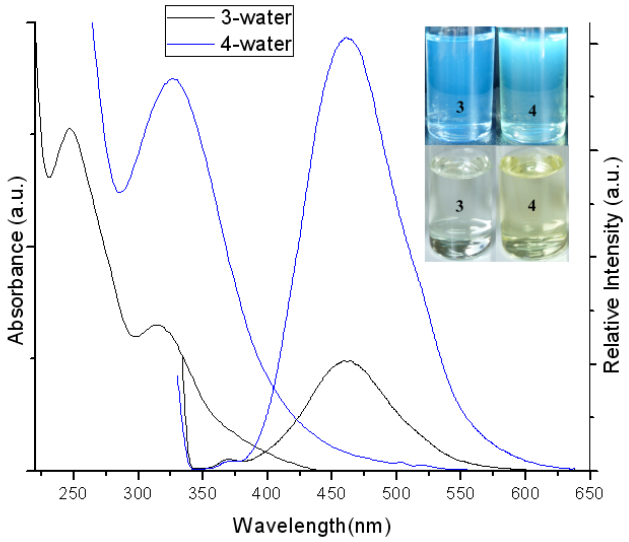

Fig. 2. UV-vis (left side) and fluorescence (right side) traces of polymers in water. The foto in the inset represents the water solutions of (**3**) and (**4**) in the day light and under excitation with a 365 nm UV lamp

It was already reported that the spectroscopic properties of the conjugated polymers nanoparticles are size-dependent [36, 37]. Therefore, it was emphasized that the red shift of the λ_{max} em increase with the particle size [36] and the fluorescence intensity decrease with the increasing of the particle size [37]. If the λ_{max} em values reported in table 3, are analysed in conjunction with the nanoparticles size obtained by DLS measurements, it can be concluded that a similar behaviour occurs for the synthesized polythiophenes (**3**) and (**4**). The increased fluorescence intensity as the size of the nanoparticles decreased was attributed to the variation of the total emitting area concomitantly with a self-absorption effect [37]. As observed in table 3, both polythiophenes present also high values of Stokes shift, which is one of the most important requests for a fluorescent compound to be used in fluorescence bioimaging [38].

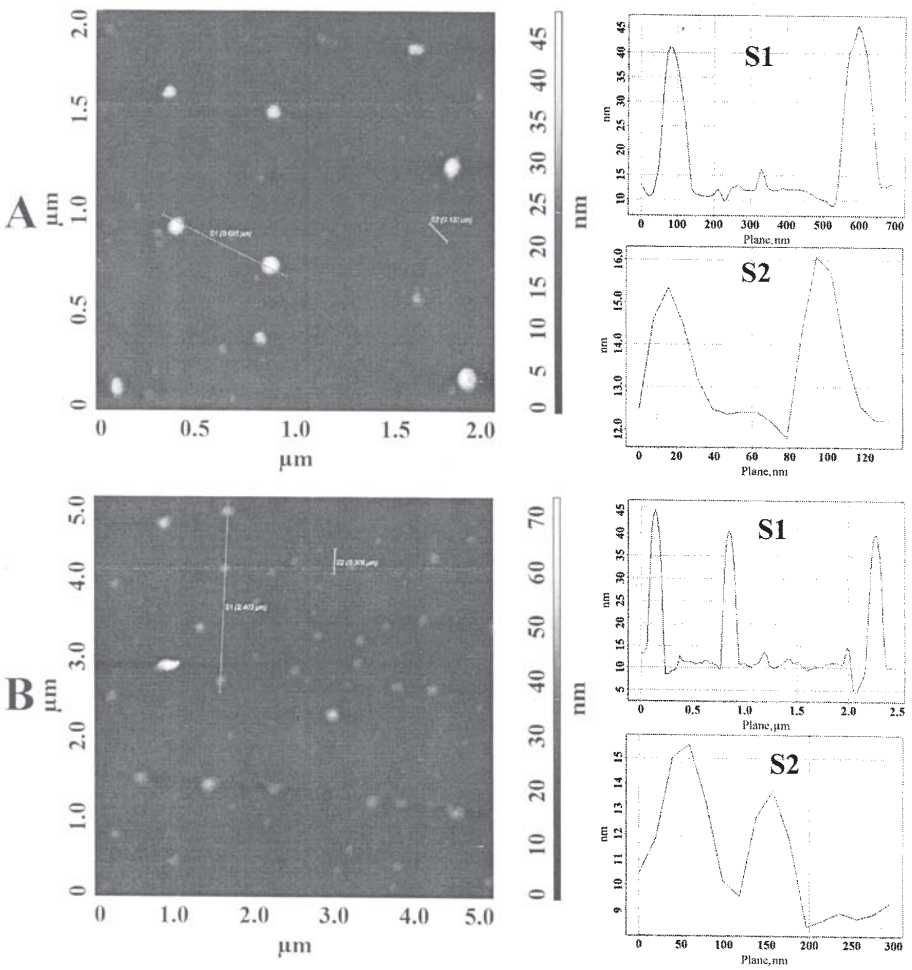

Fig. 3. Tapping-mode AFM images and cross-sectional analysis of (A) - (**3**) and (B)-(**4**)

Self-Assembly Properties in Aqueous Solutions

To study the self-assembling of the amphiphilic synthesized polythiophenes in water and to characterize the formed core-shell nanoparticles in terms of size and shape, DLS and AFM techniques were complementary used. DLS allow for the dimensional analysis of the nanoparticles in the solvated state, while AFM give an image of their shape and size in dried form. From the data presented in table 3 it can be emphasized that, as expected, for the nanoparticles formed by self-assembling during the simple dissolution in water of the synthesized polythiophenes, a higher value for hydrodynamic diameter was obtained for the copolymer (**3**), which has PEG 2000 as side chains, than that of the copolymer (**4**) which contains PEG 1000 as side chains. Having a similar PEG side chains density on the main chain, the obtained results can be explained only by the difference in the amount of the "structured water" formed around the flexible PEG side chains in the nanoparticles shell through hydrogen bonds between the oxygen ether linkages in structural units of PEG and water molecules. Therefore, when the side chains are longer, the size of nanoparticles is bigger. The nanoparticles size values obtained from AFM imaging must be taken into consideration with care because during the drying process PEG corona is collapsed and, moreover, other aggregated features might be developed due to solution over-saturation, as well as due to the interactions between nanoparticles on the one hand and nanoparticles and the substrate on the other hand.

Indeed, in figure 3 (A and B left side), tapping-mode AFM images of both copolymers show populations of nanoparticles with different size embedded in a layered morphology. The diameter values for the smallest and the biggest spherical nanoparticles were taken from the width of the peak at the baseline in cross-sectional height profiles (fig. 3 A, B right side). For polythiophene (**3**) the nanoparticles diameter size varies between 45 nm (fig. 3A-S2) and 135 nm (fig. 3A-S1). While the nanoparticles with the diameter of 45 nm derives from the formed nanoparticles in solution, the nanoparticles with 135 nm and those having size between these two values are formed due to aggregation during the freeze drying. In the case of polythiophenes (**4**) having the PEG 1000 as side chains, only the nanoparticles with the size higher than those determined by DLS were observed (fig. 3B). Their size is ranging between 120 nm and 175 nm. The different behaviour of these two polymers could be due to their different crystallization process, as is revealed by their different melting points in table 2. The dimensions of the nanoparticles of investigated polymers, as determined by DLS, were found to be in the proper range to avoid fast renal clearance (D_H > 10 nm) and still below the cut-off size of the leaky pathological microvasculature of hypervascular tumours (D_H < 200 nm) [39], thus making them candidates for application in fluorescence imaging based on the enhanced permeability and retention (EPR) effect.

In vitro cytotoxicity test of water self dispersible polythiophenes

Recent articles in the biomedical field reveal the potential use of fluorescent conjugated nanoparticles as bioactive materials. As biocompatibility is the common property requested for all biomaterials, the cytotoxicity test is the first step toward assessing the biocompatibility of a biomaterial. Thus, the cytotoxicity of fluorescent amphiphilic water-self dispersible polythiophenes (**3**) and (**4**) was evaluated by using the classical MTT cell-viability

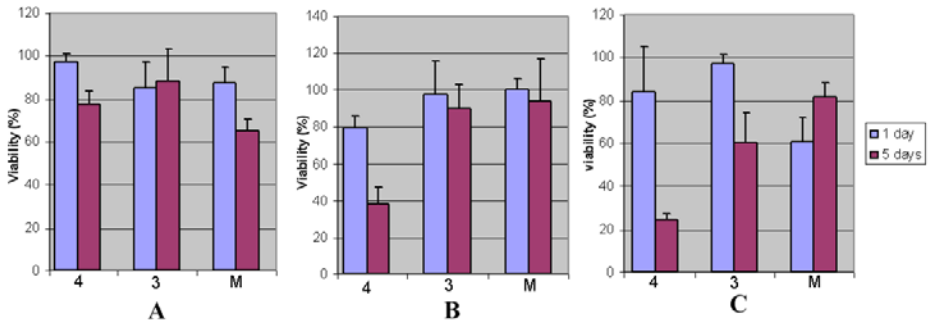

Fig. 4. Cytotoxicity of MG 63 (A), HTB11(B) and HTB 14(C) in the presence of nanoparticles

assay in which the conversion of soluble MTT into formazan is directly related to mitochondrial activity and, subsequently, to cell viability [33]. The cytotoxicities of polymers (**3**) and (**4**) were evaluated toward two different kind of human cancer cell lines (neuroblastoma HTB11 and HTB14 glioma cell line) and one normal cell line (MG 63 osteoblast). Figure 4 shows the cell viabilities after their incubation with polymers solutions at a concentration of 0.016 mg/mL for 24 and 120 h, respectively. Taking into account that the cell viabilities percentage were expressed by the ratio of absorbance of the cells incubated with polymers (**3**) or (**4**) to that of the cells incubated only with the culture medium, both polymers shows the viabilities closed or even higher to that of the controls after 24 h, thus indicating their cytocompatibility. The obtained results are consistent with the previous studies referring to other conjugated polymers (such as polyaniline, polypyrrole, and polythiophene derivatives) used for biomedical applications. [4]. The good cytocompatibility of (**3**) and (**4**) results as a consequence of their structural peculiarity. Therefore, the nanoparticles formed in aqueous solutions have the outer shell composed of hydrophilic PEG, which works concomitantly as a biomimetic surface and also as a stealth surface, which suppress the nonspecific interactions with biomolecules. The time effect of the fluorescent nanoparticles on the viability of these cell lines was also evaluated. As follows, after a period time of 5 days of incubation the viabilities percents of MG 63 osteoblasts-like cells are higher when the polymers (**3**) and (**4**) are present in the culture medium in respect to the control (fig. 4 A), indicating not only their lack of toxicity, but their capacity to promote the growth of these cells, as well. In case of cancers cells, after five days of incubation, a lower viability compared to control was registered in the presence of both polymers (fig .4 B, C).

Moreover, lower values of the viability of both HTB11 and HTB14 in the presence of polymer (**4**) were registered, as compared to those obtained in the presence of polymer (**3**). A possible explanation for such behaviour could be related to the size of the nanoparticles (table 3), which is directly related to the PEG side chains length. Therefore, in a similar amount (by weight) of polymers, a higher number of nanoparticles as well as a higher amount of polythiophene are expected for (**4**) than for (**3**). The smaller size of copolymer (**4**) nanoparticles can facilitate their cell internalization in a higher amount than that for the copolymer (**3**), being well known that PEG with a molecular weight less than 2KDa has no effect on reducing the nonspecific cellular uptake [40]. As anticancer activity of various oligo- and polythiophenes was recently reported [22, 23], it seems that a similar behaviour could be emphasized for the present investigated polythiophenes, which can motivate the observed differences of HTB11 and HTB 14 cell viability in the presence of the studied copolymers. Furthermore, a selective cytotoxicity to cancer cells over MG 63 osteoblasts-like normal cells was obtained. *In vitro* cytotoxicity results demonstrate the cytocompatibility of the studied copolymers (**3**) and (**4**), their capacity to stimulate the growth of osteoblast like cells and the inhibition of the cancer cells. All these preliminary results motivate our further studies regarding the application of fluorescent amphiphilic polythiohens (**3**) and (**4**) for both cell-imaging and cancer therapy.

Conclusions

Two water-self dispersible polythiophenes containing PEG side chains were synthesized by using the versatile thiophene chemistry and they were structurally characterized. Due to the amphiphilic character, these polymers can form stable micelle-like aggregate by self-assembling in water used as PEG selective solvent. Absorbance and emission spectra of polythiophenes nanoparticles highlight their suitability for biological imaging, the broad absorption spectra providing flexibility in the choice of excitation wavelength. Also their size, cytocompatibility, as well as the growth inhibition of the cancer cells recommend these polythiophenes as multifunctional platforms for therapy and diagnosis.

Acknowledgement: One of the authors (A. D. B.) acknowledge the financial support given by European Social Fund „Cristofor I. Simionescu" Postdoctoral Fellowship Programme (ID POSDRU/89/1.5/S/55216), Sectorial Operational Programme Human Resources Development 2007 – 2013.

References

1. PRASAD RAO, J., GECKELER, K. E., Prog. Polym. Sci., **36**, nr. 7, 2011, p. 887.
2. GUIMARD, N.K., GOMEZ, N., SCHMIDT, C. E., Prog. Polym. Sci., **32**, nr. 8-9, 2007, p. 876.
3. RAVICHANDRAN, R., SUNDARRAJAN, S., VENUGOPALL, J. R., MUNKERJEE, S., RAMAKRISHNA, S., J. R. Soc. Interface, **7**, nr. 51(supl_5), 2012, p. S 559.
4. BENDREA, A.-D., CIANGA, L., CIANGA, I., J. Biomat. Appl., **26**, no. 1, 2011, p. 3.
5. INZELT, G., J. Solid State Electrochem., **15**, nr. 7-8, 2011, p. 1711.
6. GRIMSDALE, A. C., CHAN, K. L., MARTIN, R. E., JOKISZ, P. G., HOLMES, A. B., Chem. Rev., **109**, nr. 3, 2009, p.897.
7. LI, C., LIU, M., PSCHIRER, N. G., BAUMGARTEN, M., MULLEN, K., Chem. Rev., **110**, nr. 11, 2010, p. 6817.
8. CHENG, Y.-J., YANG, S.-H., HSU, C.-H., Chem. Rev., **109**, nr. 11, 2009, p. 5868.
9. AMB, C. M., DYER, A. L., REYNOLDS, J. R., Chem. Mater., **23**, nr. 3, 2011, p. 397.
10. TUNCEL, D., DEMIR, H. V., Nanoscale, **2**, nr. 4, 2010, p. 484.
11. PECHER, J., MECKING, S., Chem. Rev., **110**, nr. 10, 2010, p. 6260.
12. KAESER, A., SCHENNING, A. P. H. J., Adv. Mater., **22**, nr. 28, 2010, p. 2985.
13. KIM, H.-J., KIM, T., LEE, M., Acc. Chem. Res., **44**, nr. 1, 2011, p. 72.
14. WEGNER, G., Thin Solid Films, **216**, nr. 1, 1992, p. 105.
15. WEGNER, G, Turkish J. Chem, **21**, 1997, p. 6.
16. WEGNER, G, Macromol. Chem. Phys., **204**, nr. 2, 2003, p. 347.
17. CIANGA, I., YAGCI, Y., Prog. Polym. Sci., **29**, nr. 5, 2004, p. 387.

18. CIANGA, I., CIANGA, L., YAGCI, Y. In New trends in nonionic (co) polymers and hybrids; Dragan, E. S., Ed.; Nova Science Publishers: New York, 2006; p 1.
19. *** Handbook of Thiophene-based Materials: Applications in Organic Electronics and Photonics, PEREPICHKA, I. F., PEREPICHKA D. F., Eds. John Wiley and Sons, 2009.
20. MISHRA, R., JHA, K. K., KUMAR. S., TOMER, I., Der Pharma Vhemica, **3**, nr. 4, 2011, p. 38.
21. D'AURIA, M., Photochemical and Photophysical Behavior of Thiophene. In: Alan R. Katritzky, editors: Advances in Heterocyclic Chemistry, Vol 104, Oxford: Academic Press; 2011, p. 127.
22. LIU, L., YU, M., DUAN, X., WANG, S., J. Mater. Chem., **20**, nr. 33, 2010, p. 6942.
23. YANG, G., LIU, L., YANG, Q., LV, F., WANG, S., Adv. Funct. Mat. **22**, nr. 4, 2012, 736.
24. XING, C., LIU, L., TANG , H., FENG , X., YANG, Q., WANG, S., BAZAN, G. C., Adv. Funct. Mater., **21,** nr. 21, 2011, p. 4058.
25. CIANGA, I., MERCORE, V. M., GRIGORAS, M., YAGCI, Y., J. Polym. Sci: Part A: Polym. Chem., **45**, nr. 5, 2007, p. 848.
26. SAHIN, E., CAMURLU, P., TOPPARE, L., MERCORE, V. M., CIANGA, I., YAGCI, Y., J. Electroanal. Chem., **579**, nr. 2, 2005, p. 189.
27. CIANGA, L., YAGCI, Y., J Polym. Sci: Part A: Polym. Chem., 40, nr. 8, 2002, p. 995.
28. PAPILA, Ö., TOPPARE, L., YAGCI, Y., CIANGA, L., Int. J. Polym. Anal. Charact., **9**, nr. 1-3, 2004, p. 13.
29. CAMURLU, A. M., YILMAZ, P. F., CIANGA, L., YAGCI, Y, TOPPARE, L., J. Appl. Polym. Sci., **102**, nr. 5, 2006, p. 4500.
30. GOEN COLAK, D., CIANGA, I., ODACI DEMIRKOL, D., KOZGUS, O., ILKER MEDINE, E., SAKARYA, S., UNAK, P., TIMUR, S., YAGCI, Y., J. Mater. Chem., **22**, nr. 18, 2012, p. 9293.
31. YUKSEL, M., GOEN COLAK, D., AKIN, M., CIANGA, I., KUKUT, M., ILKER MEDINE, E., CAN, M., SAKARYA, S., UNAK, P., TIMUR, S., YAGCI, Y., Biomacromolecules, **13**, nr. 9, 2012, p. 2680.
32. BENDREA, A.-D., CIANGA, L., HITRUC, E.-G., CIANGA, I., Int. J. Polym. Anal. Charact., in press DOI: 10.1080/ 1023666X.2013.7555598
33. MOSMANN, T., J. Immunol. Methods, **65**, 1983, p. 55.
34. POMERANTZ, M., YANG, H., CHENG, Y., Macromolecules, **28**, nr. 17, 1995, p. 5706.
35. LIAO, S.-C., LAI, C.-S., YEH, D.-D., HABIBUR RAHMAN, M., HSU, C.-S., CHEN, H.-L., CHEN, S.-A., Reac. Funct. Polym., **69**, nr. 7, 2009, p. 498.
36. GREY, J. K., KIM, D.Y., NORRIS, B. C., MILLER, W. L., BARBARA, P. F., J. Phys. Chem. B, **110**, nr. 1, 2006, p. 25568.
37. LEE, S. J., LEE, J. M., CHO, H.-Z., KOH, W.G., CHEONG, I. W., KIM, J. H., Macromolecules, **43**, nr. 9, 2010, p. 2484.
38. PALAMA, I., DI MARIA, F., VIOLA, I., FABIANO, E., GIGLI, G., BETTINI, C., BARBARELLA. G., J. Am. Chem. Soc., **133**, nr. 44 , 2011, p. 17777.
39. JÄGER, E., JÄGER, A., ETRYCH, T., GIACOMELLI, F. C., CHYTIL, P., JIGOUNOV, A., PUTAUX, J. L., RIHOVÁ , B., ULBRICH, K., ŠTEPÁNEK, P., Soft Matter, **8**, nr. 37, 2012, p. 9563.
40. JOKERST, J. V., LOBOVKINA, T., ZARE, R. N., GAMBHIR, S. S., Nanomedicine, **6**, nr. 41, 2011, p. 715

Manuscript received: 11.03.2013